J. Am. Chem. Soc. 1991, 113, 4741–4746

Mechanistic and Kinetic Studies of the Reactions of Gas-Phase Methyl Radicals with Metal Oxides

Youdong Tong and Jack H. Lunsford*

Contribution from the Department of Chemistry, Texas A&M University, College Station, Texas 77843. *Received November 27, 1990*

Abstract: Reactions of $CH_3^•$ radicals with metal oxide powders have been studied quantitatively for the first time in an attempt to understand the very large differences in selectivity that occur during the catalytic oxidation of methane. The sticking coefficients for $CH_3^•$ radicals on ZnO, CeO_2, and MgO were determined to be 1.8×10^{-5}, 2.1×10^{-6}, and 1.2×10^{-7}, respectively. The relative specific reaction rates of $CH_3^•$ radicals with metal oxides were found to follow the series ZnO > MoO_3 > NiO > CeO_2 > MgO $\simeq$ Li^+/MgO. From the absolute sticking coefficients and the relative reaction rates, first-order rate constants for the $CH_3^•$ radical reactions with metal oxides were determined. Methyl radicals react with MoO_3/SiO_2 by electron transfer, which is apparent in the reduction of Mo^{6+} to Mo^{5+}. An analogous reaction apparently occurs on CeO_2 at 100 °C, but the electron is subsequently transferred to molecular oxygen, forming O_2^- on the surface. As a result of this reduction reaction, methoxide ions are produced, and these yield formate ions. The methoxide and formate ions are believed to be intermediates in the nonselective oxidation of CH_4 to CO and CO_2. For the selective oxidative dimerization of CH_4, a small sticking coefficient is required so that a $CH_3^•$ radical may reflect off a catalyst surface many times before it collides and reacts with another $CH_3^•$ radical. Thus, ZnO, MoO_3, NiO, and CeO_2 are nonselective oxidation catalysts, whereas Li^+/MgO is a reasonably active and selective catalyst for the oxidative dimerization reaction.

Introduction

The role of surface-generated gas-phase $CH_3^•$ radicals as intermediates in the formation of ethane during the oxidative dimerization of methane is now well-established.[1,2] It also is known that, at $T < 700$ °C, the nonselective oxidation products CO and CO_2 (CO_x) are formed by the direct oxidation of methane rather than by the oxidation of secondary products C_2H_4 and C_2H_6.[3] The mechanism by which this direct oxidation occurs, however, has only been a matter of speculation. One of the main pathways leading to the formation of CO_x is believed to be via secondary reactions of the gas-phase $CH_3^•$ radicals with the catalytic metal oxide surfaces.[4] The potential importance of this reaction pathway in the oxidation of methane is apparent if one considers that a given methyl radical will collide ca. 10^5 times with a metal oxide surface before it reacts with another $CH_3^•$ radical in the gas phase.[5]

Although similar reactions between radicals and surfaces probably play a role in many hydrocarbon oxidation processes, very little information is available on them, and they are generally referred to as "wall effects". In our previous study, an inverse correlation was found between the rate of appearance of $CH_3^•$ radicals over selected lanthanide oxides and the rate at which $CH_3^•$ radicals reacted with these oxides.[4] The greater reactivities of the oxides of Ce, Pr, and Tb were attributed to the redox properties of these three oxides; i.e., they exhibit multiple oxidation states that make them accessible to reduction by $CH_3^•$ radicals. This observation led to the suggestion that the reaction of $CH_3^•$ radicals with a metal oxide may occur through electron transfer with the concomitant formation of a methoxide ion:

$$M^{(n+1)+}O^{2-} + CH_3^•(g) \rightarrow M^{n+}(OCH_3)^- \qquad (1)$$

The present study was undertaken to determine the kinetics and the mechanism for the reactions of $CH_3^•$ radicals with metal oxide surfaces. Six representative metal oxides, MoO_3 (or MoO_3/SiO_2), CeO_2, ZnO, NiO, MgO, and Li^+/MgO, were used in this study. The first four oxides can be rather easily reduced, whereas MgO and Li^+/MgO cannot. Li^+/MgO is one of the more selective catalysts for the oxidative dimerization of CH_4.[6] It is capable of generating gas-phase $CH_3^•$ radicals, but previous work has demonstrated that it does not react with $CH_3^•$ radicals nor does it promote the coupling of $CH_3^•$ radicals.[7] The catalysts MoO_3/SiO_2 was of special interest because the reduction of Mo^{6+} to Mo^{5+} could be followed by ESR spectroscopy.

Experimental Section

CeO_2 (99.9%), ZnO (99.999%), NiO (99.99%), MoO_3 (99.99%), and MgO (99.9%) were obtained from Aldrich. The MgO and other oxides were calcined at 1100 and 550 °C, respectively, in air for 10 h. The 7 wt % Li^+/MgO and the 2 wt % MoO_3/SiO_2 were prepared according to the methods described in the literature.[6,8] The silica gel, grade 57, was obtained from Davison Specialty Chemical Co. Before exposure to reactants, all the materials were further treated in flowing O_2 (50 mL min^{-1}) at 500 °C for 2 h.

The reactions of the gas-phase $CH_3^•$ radicals with metal oxides were conducted in a reactor coupled with a matrix isolation electron spin resonance (MIESR) system, which has been described previously in detail.[9] The collection–detection efficiency of the system was determined with use of NO_2 as the calibration gas. Thus, the concentration of methyl radicals could be quantitatively determined.[10] The flow reactor and the experimental method were modified for the specific purpose of each experiment. The flow rates of gases (at STP) were as follows: Ar, 3.7 mL min^{-1}; CH_4, 1.1 mL min^{-1}; O_2, 0.025 mL min^{-1}.

Kinetic Study. The method for determination of the relative reactivities of metal oxides toward $CH_3^•$ radicals has been described in detail in our previous study.[4]

Sticking coefficients and activation energies were determined over selected metal oxides with the use of the modified reactor shown in Figure 1. The metal oxide (scavenger) was located after the gas leak in the collection–detection region of the MIESR system instead of before the gas leak. With this configuration, the temperature of the metal oxide could be adjusted separately from that of the generator, and the pressure within the metal oxide region was sufficiently low so that the collisions between gas-phase molecules were greatly reduced. During an experiment, the total gas flow was directed through the leak and over the scavenger.

A layer of Sm_2O_3 chips was used as the $CH_3^•$ radical generator, and the metal oxide (scavenger) also was in the form of chips. The metal oxide chips were uniformly distributed between two layers of quartz wool. Experimental measurements showed that a 2 order of magnitude drop in pressure resulted from the bed (the two layers of quartz wool with metal oxide chips); however, it was found that the second layer of quartz

---

[1] Lunsford, J. H. *Langmuir* **1989**, *5*, 12–16.
[2] Lunsford, J. H. *Catal. Today* **1990**, *6*, 235–259.
[3] Nelson, P. F.; Cant, N. W. J. *Phys. Chem.* **1990**, *94*, 3756–3761.
[4] Tong, Y.; Rosynek, M. P.; Lunsford, J. H. *J. Phys. Chem.* **1989**, *93*, 2896–2898.
[5] Tong, Y. Ph.D. Dissertation, Texas A&M University, 1991.
[6] Ito, T.; Lunsford, J. H. *Nature* **1985**, *314*, 721–722.
[7] Campbell, K. D.; Lunsford, J. H. *J. Phys. Chem.* **1988**, *92*, 5792–5796.
[8] Liu, H.-F.; Liu, R.-S.; Liew, K. Y.; Johnson, R. E.; Lunsford, J. H. *J. Am. Chem. Soc.* **1984**, *106*, 4117–4121.
[9] Martir, W.; Lunsford, J. H. *J. Am. Chem. Soc.* **1981**, *103*, 3728–3732.
[10] Campbell, K. D.; Morales, E.; Lunsford, J. H. *J. Am. Chem. Soc.* **1987**, *109*, 7900–7901.

0002-7863/91/1513-4741$02.50/0

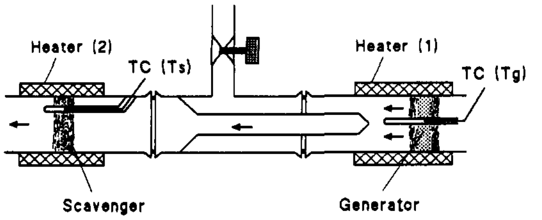

Figure 1. Reactor for kinetic studies of the reactions of methyl radicals on metal oxides.

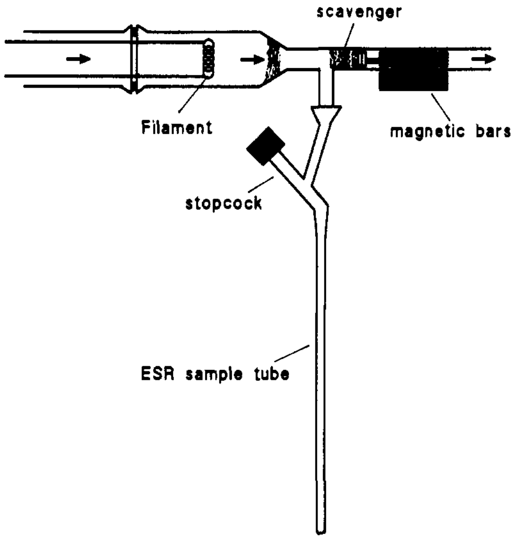

Figure 2. Apparatus for ESR spectroscopic characterization of the metal oxides.

wool, or more correctly the effect of pumping on the downstream side of the bed, was mainly responsible for this pressure drop. The pressure gradients across the layer of metal oxide chips and the first layer of quartz wool were negligible relative to the total pressure drop. The pressure in the region between the two layers of quartz wool was measured to be $(8.0 \pm 0.5) \times 10^{-2}$ Torr. The pretreatment and the reaction were under the same conditions as in the experiments mentioned above. Blank experiments demonstrated that the quartz wool was responsible for the loss of only 4% of the $CH_3^\bullet$ radicals.

The sticking coefficient is defined as the ratio of the number of the $CH_3^\bullet$ radicals reacted on a metal oxide to the number of the collisions between $CH_3^\bullet$ radicals and the metal oxide. The former came directly from the MIESR measurement, and the latter was calculated on the basis of the partial pressure of the gas-phase $CH_3^\bullet$ radicals, which was obtained from the MIESR measurement as well. The sticking coefficients were determined over 0.050 g of 45–80 mesh ZnO chips and 0.30 g of 20–40 mesh CeO_2 or MgO chips. In a typical experiment, the metal oxide was exposed to a known partial pressure of $CH_3^\bullet$ radicals for 15 min in the flow reactor. The concentration of radicals was ca. 6×10^{17} $CH_3^\bullet$ m^{-3}. The number of radicals that reacted during this period was determined by measuring the integrated difference between the flux of radicals that entered and exited the metal oxide zone. This value was compared with the total number of collisions between $CH_3^\bullet$ radicals and the metal oxide during this period. The total number of the collisions was determined by the following equation:[11]

$$N = \frac{p}{(2\pi m k_B T)^{1/2}} \mathrm{SA}t \qquad (2)$$

where p is the partial pressure of methyl radicals, which was determined from measurement of the total pressure and the concentration of methyl radicals in the reaction region; SA is the total surface area of the metal oxide used; t is the reaction time; m is the molecular weight of $CH_3^\bullet$ radicals; k_B is the Boltzmann constant; and T is the reaction temperature. It is important to note that the reaction time is the total time of the radical collection, i.e. the time that the metal oxide was exposed to a partial pressure, p, of $CH_3^\bullet$ radicals. Thus, the fact that some of the $CH_3^\bullet$ radicals may have bypassed the metal oxide particles is not a problem.

Table I. Relative Specific Reaction Rates

oxide	amt, g	surface area, $m^2\ g^{-1}$	relative specific rate,[a] $CH_3^\bullet\ m^{-2}\ s^{-1}$
ZnO	0.050	0.03	150
MoO_3	0.15	0.58	129
NiO	0.050	1.2	63
CeO_2	0.050	2.4	18
MgO	0.15	14.9	0.9
Li^+/MgO	0.20	2.7	1.1

[a] Temperature 470 °C.

Table II. Rate Constants, Activation Energies, and Sticking Coefficients

oxides	k^a, $s^{-1}\ m^{-2}$	E_a, kcal mol^{-1}	S^a
MgO	3.0×10^2	5.7	1.2×10^{-7}
CeO_2	3.1×10^3		2.1×10^{-6}
NiO	2.1×10^4		
MoO_3	4.3×10^4		
ZnO^b	4.4×10^4	2.6	1.8×10^{-5}

[a] T = 482 °C. [b] The surface area of this ZnO was 5.2 $m^2\ g^{-1}$; those of the other oxides were the same as listed in Table I.

In the measurement of activation energy, the temperature of the metal oxide was varied between 330 and 400 °C over ZnO and 200 and 500 °C over MgO; 0.050 g of ZnO and 0.25 g of MgO were used in the measurements. For a given oxide, reactivities at several temperatures were measured, and the metal oxide was regenerated by calcining in O_2 between each reaction temperature.

ESR Characterization. The reactor, shown in Figure 2, was used for detection by ESR of paramagnetic ions formed in metal oxides as a result of reaction with the gas-phase $CH_3^\bullet$ radicals. The ESR sample tube was connected to the reactor via a ball joint. A metal oxide (scavenger) in the amount of 0.10 g was supported between two layers of quartz wool. A magnetic bar, sealed in a piece of glass tube, was connected to a quartz frit so that the quartz frit was movable along the reactor. Quartz wool, located between the generator and the metal oxide, served to remove thermal energy from activated methane molecules. The radical generator was a filament coated with a thin film of Sm_2O_3.

The metal oxide was pretreated in flowing O_2 at 450 °C for an additional 2 h. After the O_2 flow was stopped, the temperature was lowered to the desired value while evacuating the gas for 10 min. The reactant mixture was then introduced to the system. The total pressure in the reactor was about 0.5 Torr. After 50 min of reaction, the flow of reactants was terminated and the pressure in the reactor was increased to about 1 atm by adding Ar. Under the Ar atmosphere, the metal oxide chips were transferred into the ESR tube and sealed in the tube by closing the stopcock. The sample tube was removed from the MIESR system and cooled to 77 K, and spectra were recorded by using a Varian E-6S ESR spectrometer.

IR Spectroscopic Study. The surface intermediates formed on a metal oxide during reaction were identified by IR spectroscopy. The IR cell, which contained a movable wafer holder, was connected to the reactor via an O-ring joint. The wafer was made from the metal oxide of interest, and the radical generator was either Sm_2O_3 chips or a filament coated with a thin film of Sm_2O_3. The temperature of the wafer was controlled and measured via a thermocouple positioned at the outside of the reactor, adjacent to the wafer. The pressure in the reactor was about 10^{-2} Torr.

The pretreatment and the reaction were carried out in the same manner as described in the preceding experiment. The wafer was located in the reactor and positioned such that it was perpendicular to the gas flow from the generator. After 60 min of reaction, the wafer was lifted into the IR cell. The reactant flow was terminated, and Ar was admitted to raise the pressure in the system. When the pressure was more than 1 atm, the stopcock at the top of the IR cell was open to air. Helium flow was then introduced into the system via the O-ring joint attached to the stopcock. Under the He as well as Ar flow, the IR cell was disconnected from the reactor and sealed at the bottom by attaching a closed tube to the O-ring joint and at the top by closing the stopcock. The IR cell was mounted in the sample compartment of a Perkin-Elmer Model 1710 FTIR spectrometer. IR spectra were recorded with a resolution of 2 cm^{-1}.

Results

The reactivities of the selected metal oxides toward $CH_3^\bullet$ radicals were determined at 470 °C, and the results are reported

---

(11) Jordan, P. C. *Chemical Kinetics and Transport*; Plenum Press: New York, 1979; Chapter 1.

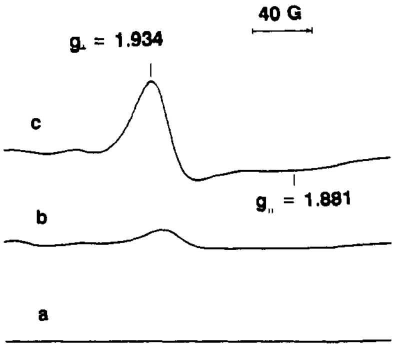

Figure 3. ESR spectra of 2% MoO_3/SiO_2: (a) untreated; (b) after exposure to flowing CH_4 and O_2 plus a small concentration of $CH_3^\bullet$ radicals at 25 °C for 90 min; and (c) after exposure to the reactants containing a high concentration of methyl radicals at 25 °C for 90 min.

in Table I in terms of their relative specific reaction rates (per unit surface area). The reaction rates differed by more than a factor of 150.

The sticking coefficients measured over ZnO, CeO_2, and MgO are reported in Table II. We believe that these are the first sticking coefficients that have been determined for reactions between $CH_3^\bullet$ radicals and a metal oxide surface. The results of the sticking coefficient measurement are consistent with the results obtained from the relative specific reactivity measurements. The error in the reported sticking coefficients is estimated to be ±50%. The rate constants for the reaction of methyl radicals on selected oxides are also given in this table. The rate constants for ZnO and CeO_2 were calculated on the basis of their sticking coefficients and the concentration of $CH_3^\bullet$ radicals in the metal oxide region. The rate constants for other oxides in the table were obtained from comparisons of their specific reactivities relative to that of CeO_2.

It is evident from the results of Tables I and II that the relative specific rates of reaction for the two ZnO samples, which had very different surface areas, were nearly equivalent. For example, both ZnO samples exhibited a rate of reaction per meter squared that was about 150 times greater than that observed over MgO. These results indicate that radical transport into the metal oxide particles was not a problem. That is, there was no significant concentration gradient from the external to the interal regions of the particle, even with the most active metal oxide.

One of the assumptions in the calculation of the rate constants was that the reaction rate was first-order in the concentration of $CH_3^\bullet$ radicals. The assumption was justified by an experiment in which glass beads coated with a thin CeO_2 film (the glass beads were 3 mm in diameter, and each bead contained about 1.9×10^{-4} g of CeO_2) were used in place of the metal oxide chips. When the number of beads packed in the reactor was changed, the relative reaction rates corresponding to different residence times were obtained. A plot of the logarithm of the $CH_3^\bullet$ radical concentration versus the number of beads exhibits a good linear relationship. This is expected if the reaction rate is first-order in the concentration of $CH_3^\bullet$ radicals.

The activation energies of the reactions over ZnO and MgO are reported in Table II. It was found that the reaction rates were slightly dependent on temperature, and even at ambient temperature ZnO exhibited a measurable reactivity toward $CH_3^\bullet$ radicals.

To determine whether the oxidation states of the metal cations in a metal oxide decreased as a result of a reaction with $CH_3^\bullet$ radicals, the paramagnetic properties of two of the most reactive materials, 2% MoO_3/SiO_2 and CeO_2, were investigated with the use of ESR spectroscopy. The ESR spectra shown in Figure 3 were obtained with the 2% MoO_3/SiO_2 samples treated under different conditions. Spectrum a was obtained with an untreated MoO_3/SiO_2 sample, and spectrum c was recorded after the untreated sample had been exposed to reactants containing methyl radicals and methane at 25 °C. As a comparison, spectrum b was obtained with the MoO_3/SiO_2 sample, which had been treated in the same way as that of spectrum c but with the $CH_3^\bullet$ generator being replaced by a layer of heated quartz wool. In this case, the concentration of $CH_3^\bullet$ radicals in the reactants was greatly reduced compared with that in the case of spectrum c. The Mo^{5+} ions, characterized by $g_\perp = 1.934$ and $g_\parallel = 1.881$,[12] were found in both spectra c and b, but the concentration of Mo^{5+} was much greater in the sample that had been exposed to a large concentration of $CH_3^\bullet$ radicals. This indicates that the reduction of Mo^{6+} to Mo^{5+} took place during both treatments c and b but that the methyl radicals were mainly responsible for the formation of the Mo^{5+} ions observed in spectrum c.

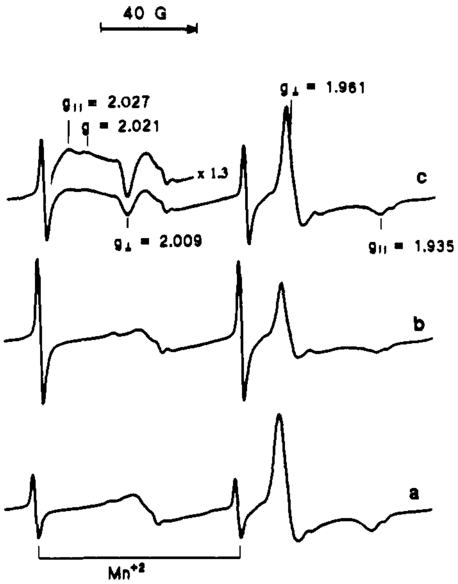

Figure 4. ESR spectra of CeO_2: (a) untreated; (b) after exposure to flowing CH_4 and O_2 plus a small concentration of $CH_3^\bullet$ radicals at 100 °C for 90 min; and (c) after exposure to the reactants containing a high concentration of methyl radicals at 100 °C for 90 min.

Similar experiments were carried out with CeO_2. At 25 °C, there was no detectable change in the ESR spectrum for the samples treated under two different conditions. However, as shown in Figure 4, at 100 °C, a species characterized by $g_\parallel = 2.027$ and $g_\perp = 2.009$ was found only in spectrum c, which corresponds to the sample exposed to the greater concentration of methyl radicals. The new spectrum is attributed to superoxide ions, O_2^-, on CeO_2.[13] The small maximum at $g_\parallel = 2.021$ in spectrum c is probably a result of O_2^- ions at a different environment on the surface. The reduction of manganese impurities to Mn^{2+} was observed in both spectra b and c, and thus $CH_3^\bullet$ radicals or other hydrocarbon impurities were mainly responsible for this reduction. The decrease in the concentration of the species responsible for the spectrum with $g_\perp = 1.961$ and $g_\parallel = 1.935$ was noted in spectrum b, and only a slight change was observed in spectrum c relative to spectrum a. It has been argued that the signal at $g_\perp = 1.961$ and $g_\parallel = 1.935$ results from quasi-free electrons in CeO_2.[14] Although Ce^{3+} cations were expected, they could not be unambiguously identified, which may result from the spectral broadening caused by a short spin-lattice relaxation time at 77 K[14] or to the rapid transfer of electrons from Ce^{3+} to O_2.

The surface intermediates formed during the reaction of methyl radicals on CeO_2 were studied by IR spectroscopy. The C–H and C–O stretching regions of the IR spectrum of a CeO_2 sample that had reacted with methyl radicals at 25 °C are shown in Figure 5. The spectra recorded at different reaction temperatures in the region 950–1700 cm^{-1} are shown in Figure 6. The bands observed at 25 and 100 °C and their assignments are given in Table III. Methoxide and formate ions are believed to be responsible for the IR bands observed at 25 °C.[8,15–19] The presence

---

(12) Vorotyntsev, M. V.; Shvets, V. A.; Kazanskii, V. B. *Kinet. Catal.* (*Engl. Transl.*) **1971**, *12* (5), 1108–1112.

(13) Gideoni, M.; Steinberg, M. J. *Solid State Chem.* **1972**, *4*, 370–373.

(14) Steinberg, M. *Isr. J. Chem.* **1970**, *8*, 877–881.

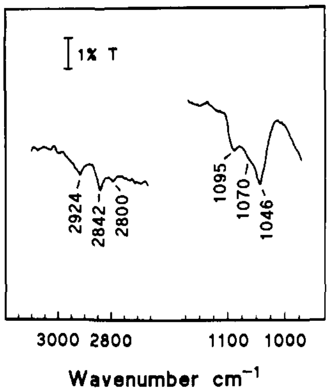

Figure 5. IR spectra of the surface species on CeO_2 following reaction with methyl radicals at 25 °C.

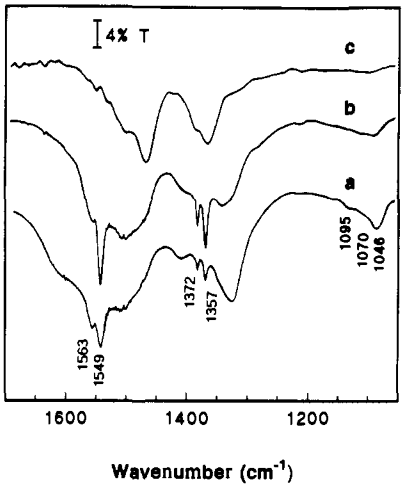

Figure 6. IR spectra of methoxide and formate ions on CeO_2 as a function of reaction temperature: (a) 25 °C; (b) 100 °C; and (c) 300 °C.

Table III. IR Spectroscopic Observations on CeO_2 after Reaction with $CH_3^•$ Radicals

temp, °C	band, cm^{-1}	intensity[a]	assignment	surface group
25	2924	w	$\nu_{C-H(as)}$	$MOCH_3$
	2842	m	$\nu_{C-H(s)}$	
	2800	w	$\nu_{C-H(s)}$	
	1095	m	ν_{C-O}	
	1070	w	ν_{C-O}	
	1549	s	$\nu_{O-C-O(as)}$	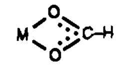
	1372	w	δ_{C-H}	
	1357	w	$\nu_{O-C-O(s)}$	
	1563	s	$\nu_{O-C-O(as)}$	
	1046	m	ν_{C-O}	?
100	2845	w	ν_{C-H}	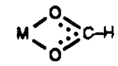
	1549	s	$\nu_{O-C-O(as)}$	
	1372	m	δ_{C-H}	
	1357	s	$\nu_{O-C-O(s)}$	

[a] Key: s = strong, m = medium, and w = weak.

of two C–O stretching bands at 1070 and 1095 cm^{-1} suggests that there were probably at least two kinds of methoxide ions. This is in agreement with the observation that three kinds of methoxide ions are present on CeO_2 during the dissociative adsorption of methanol.[17,19] With increasing temperature, the concentration of methoxide ions decreased, whereas that of formate ions increased. At 100 °C, the observed surface species were mainly formate ions. At temperatures around 200 °C, the concentration of formate ions reached a maximum, and at temperatures greater than 300 °C no formate was detected.

Blank experiments were carried out in which the radical generator Sm_2O_3 was replaced by CeO_2, which does not form $CH_3^•$ radicals. Bands were observed from the CeO_2 scavenger at 2960, 2930, and 2856 cm^{-1} along with a weak band at 1046 cm^{-1}. The bands attributed to methoxide and formate ions were not detected.

Discussion

As noted previously, metal oxides differ greatly with respect to their ability to react with $CH_3^•$ radicals. The range of activities reported in Table I is even greater than was found for the lanthanide oxides.[4] These rate constants may find application in kinetic modeling studies on the oxidative dimerization of CH_4. The results of Table I support the observation that those metal oxides having metal ions with accessible multivalent oxidation states are more reactive than those that are difficult to reduce. It is well-known that the first three oxides are more easily reduced than MgO or Li^+/MgO. Although the most stable oxidation state for zinc is 2+, ZnO is a nonstoichiometric oxide and an n-type semiconductor. The partial reduction of ZnO is facile because of the capacity of ZnO to accommodate interstitial Zn^+ ions and oxygen vacancies.[20] As might be expected from these results, ZnO is a nonselective CH_4 oxidation catalyst.[21] The lower reactivity of Li^+/MgO toward $CH_3^•$ radicals likewise is consistent with the fact that Li^+/MgO is a reasonably selective catalyst in the oxidative dimerization of methane. Therefore, all of the observations concerning the reactivities of metal oxides suggest that the reactivity of a metal oxide is related to its reducibility.

In our previous study, the high relative reactivity of a reducible metal oxide, such as CeO_2, was accounted for by a mechanism in which the interaction between methyl radicals and the metal oxide was accomplished through reaction 1. The present ESR and IR spectroscopic studies support such a mechanism. It is evident from the ESR characterization that $CH_3^•$ radicals were responsible for the reduction of metal ions in the oxides. As the spectra of Figure 3 show, the reaction of $CH_3^•$ radicals on the MoO_3/SiO_2 catalyst led to a reduction of Mo^{6+} to Mo^{5+}. Although the formation of Ce^{3+} ions could not be identified in CeO_2, the formation of the O_2^- ions on CeO_2 during reaction is an indication that electrons had been transferred from $CH_3^•$ radicals to Ce^{4+} and subsequently from Ce^{3+} to O_2. That is, O_2^- was formed via the reaction

$$O_2 + Ce^{3+} \rightarrow Ce^{4+}O_2^- \qquad (3)$$

It has been demonstrated that the interaction of gaseous molecular oxygen with reduced metal cations results in formation of O_2^- ions via electron transfer.[22] The failure to detect O_2^- on the MoO_3/SiO_2 sample probably results from the fact that the formation of the O_2^- species is reversible on this oxide.[23] At the low O_2 partial pressure of this experiment, the concentration of O_2^- apparently was too small to be detected by ESR.

Cerium oxide is a particularly suitable material for observing surface intermediates because the solid itself does not strongly absorb infrared radiation over a rather broad range of wavelengths. The bands at 1070 and 1095 cm^{-1} provide evidence for the formation of methoxide ions from $CH_3^•$ radicals. The C–H stretching bands at 2800–2924 cm^{-1} support this assignment; however, the

---

(15) Ueno, A.; Onishi, T.; Tamaru, K. *J. Chem. Soc., Faraday Trans. 1* **1971**, *67*, 3585–3589.

(16) Little, L. H. *Infrared Spectra of Adsorbed Species*; Academic Press: New York, 1966.

(17) Lemotte, J.; Moravek, V.; Bensitel, M.; Lavalley, J. C. *React. Kinet. Catal. Lett.* **1988**, *36*, 113–118.

(18) Li, C.; Sakata, Y.; Arai, T.; Domen, K.; Maruya, K.; Onishi, T. *J. Chem. Soc., Faraday Trans. 1* **1989**, *85*, 929–943.

(19) Li, C.; Domen, K.; Maruya, K-I.; Onishi, T. *J. Catal.* **1990**, *125*, 445–455.

(20) Neumann, G. Non-Stoichiometry and Defect Structure. In *Current Topics in Materials Science*; Kaldis, E., Ed.; North-Holland: New York, 1981; Vol. 7.

(21) Zhang, H.; Wang, J.; Driscoll, D. J.; Lunsford, J. H. *J. Catal.* **1988**, *112*, 366–374.

(22) Lunsford, J. H. *Catal. Rev. - Sci. Eng.* **1973**, *8*, 135–157.

(23) Che, M.; Tench, J.; Naccache, C. *J. Chem. Soc., Faraday Trans. 1* **1974**, *70*, 263–272.

latter bands are not definitive evidence. Bands in the 2856–2960 cm^{-1} region, which were previously used to establish the presence of methoxide ions,[8] were also observed in this study, following the reaction of $CH_3^{\bullet}$ radicals with MoO_3/SiO_2. But we have found that the higher wave number bands also may be produced by hydrocarbon impurities in the vacuum system. The increase in the formate ion bands at the expense of the methoxide ion bands suggests that the formate ions are derived from the methoxide ions. Formate ions have been identified as intermediates in the decomposition of methanol to CO and H_2O. Therefore, it is concluded that methoxide and formate ions are the surface intermediates formed during the reaction of $CH_3^{\bullet}$ radicals with metal oxides, and likewise these ions are intermediates in the complete oxidation of CH_4.

On the basis of the above discussion, the mechanism of the reaction of $CH_3^{\bullet}$ radicals with metal oxides is summarized as follows

$$M^{(n+1)+}O^{2-} + CH_3^{\bullet} \rightarrow M^{n+}(OCH_3)^- \tag{4}$$

$$M^{n+}(OCH_3)^- + O_2 \rightarrow M^{n+}(O_2CH)^- + H_2O \tag{5}$$

$$M^{n+}(O_2CH)^- \rightarrow M^{n+}(OH)^- + CO \tag{6}$$

$$2M^{n+}(OH)^- + {}^1\!/_2O_2 \rightarrow 2M^{(n+1)+}O^{2-} + H_2O \tag{7}$$

In addition to these reactions, the methoxide ion may decompose to form formaldehyde, which occurs during the catalytic oxidation of methanol.[8] At the temperatures employed for the oxidative coupling of methane, the complete oxidation of the formaldehyde would occur.

The low activation energies reported in Table II are not surprising considering the participation of radicals in the reaction. Activation energies of 1.4 and 4.3 kcal/mol have been found in the decay of allyl peroxide radicals over $Bi_2O_3{\cdot}MoO_3$ and MoO_3, respectively.[24] By contrast, the observed sticking coefficients were much lower than expected from the corresponding low activation energies. The apparent sticking coefficient obtained for MgO may reflect to some extent the removal of $CH_3^{\bullet}$ radicals by coupling on the surface but is much lower than that obtained on the two oxides because of chemical reaction with the surfaces, which is expected to be more efficient than the surface coupling reaction. A detailed consideration of the proposed reaction mechanism and the characteristics of the surface of a metal oxide suggests that the low activation energies and sticking coefficients may be interpreted by two alternative mechanisms.

One interpretation is that the rate-limiting step for the reaction of methyl radicals on a metal oxide is the electron transfer from a methyl radical to a metal ion. This transfer occurs via a surface lattice oxygen ion following the attachment of the methyl radical to the lattice oxygen ion.

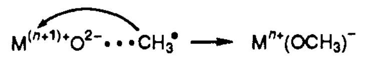

$$M^{(n+1)+}O^{2-}\cdots CH_3^{\bullet} \longrightarrow M^{n+}(OCH_3)^- \tag{8}$$

This reaction implies that methyl radicals are adsorbed on oxide ions instead of metal ions. This is likely to occur over those metal oxides that have been previously treated in O_2 at high temperatures, since the lattice of most metal oxides is terminated with oxide ions after such a treatment. For oxidized MoO_3, the Mo^{6+} ions are located in the 4-fold site below the oxide ions.[25] Thus, it is difficult for a $CH_3^{\bullet}$ radical to adsorb with its carbon in close proximity to a Mo^{6+} ion, considering the size and the orientation of a $CH_3^{\bullet}$ radical. It also has been reported than an oxygen-rich surface is formed after ZnO is treated in O_2 at temperatures higher than 650 °C.[26]

Apparently, it is difficult for the electron to penetrate through the electron cloud of the O^{2-} ion to combine with the metal ion. However, this electron transfer process may be accomplished by electron tunneling through the energy barrier caused by the O^{2-} ion. A derivation based on the theory of electron tunneling indicates that the involvement of electron tunneling in a reaction changes the kinetics of the reaction by lowering both the activation energy and the preexponential factor of the reaction.[27] Accordingly, the activation energies observed in this study are comparable with those reported for cases where electron tunneling was the dominant pathway of a reaction.[28-30] The low sticking coefficients corresponding to such low activation energies occur because of small preexponential factors. Therefore, our observation is consistent with the effect of electron tunneling on reaction kinetics.

According to this model, the sticking coefficient for the reaction of methyl radicals on a metal oxide is an indirect measurement of the probability for the electron transfer from the carbon of the radical to the metal cation via the $[M^{(n+1)+}O^{2-}\cdots CH_3^{\bullet}]$ transition complex. This probability is determined by the ratio of the lifetime of the complex (i.e., the residence time of the $CH_3^{\bullet}$ radical on the O^{2-} site) and the time for the electron transfer process. As implied, the $O^{2-}\cdots CH_3^{\bullet}$ interaction in the transition complex is believed to be very weak (possibly just van der Waals forces), so the adsorption can be approximately treated as physical condensation of methyl radicals on O^{2-} ions. On the basis of this assumption, the residence time of $CH_3^{\bullet}$ radicals on surface can be calculated by[31]

$$\tau = \tau_0 \exp(\delta H/RT) \tag{9}$$

where τ_0 is a time constant, frequently of the order 10^{-12} s, and δH is the vaporization heat of $CH_3^{\bullet}$ radicals, which can be approximated by that of methane (about 2.2 kcal/mol). A value of τ on the order 10^{-11} s is thus obtained.

The time for the electron tunneling process can be roughly estimated on the basis of the tunneling rate constants reported in the literature. In the case of intramolecular electron transfer by tunneling in organometallic compounds, rate constants of 10^3–10^6 s^{-1} are typical.[32-34] The electron transfer in the transition complex $[M^{(n+1)+}O^{2-}\cdots CH_3^{\bullet}]$ can be approximated by that in organometallic compounds. Thus, the time for electron transfer to be accomplished in the transition complex is about 10^{-3}–10^{-6} s. Compared with the residence time of the $CH_3^{\bullet}$ radical on the surface, a much longer time is needed for electron transfer. From the above comparison, the sticking coefficient for the reaction of $CH_3^{\bullet}$ radicals with a metal oxide should be in the range of 10^{-5}–10^{-8}, which just covers the observed sticking coefficients.

An alternative explanation for the observed low activation energy and sticking coefficient of methyl radicals on a metal oxide is based on the consideration of an adsorption–migration mechanism. According to this mechanism, a methyl radical initially adsorbs on a metal ion and transfers an electron and the resulting ion subsequently moves to a neighboring lattice oxygen ion through a three-center transition-state complex

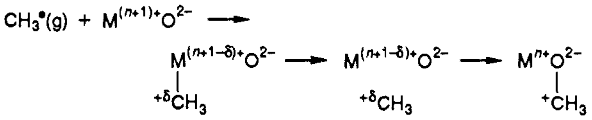

$$CH_3^{\bullet}(g) + M^{(n+1)+}O^{2-} \longrightarrow \underset{{}^{+\delta}CH_3}{M^{(n+1-\delta)+}}O^{2-} \longrightarrow \underset{{}^{+\delta}CH_3}{M^{(n+1-\delta)+}}O^{2-} \longrightarrow \underset{{}^{+}CH_3}{M^{n+}O^{2-}} \tag{10}$$

It seems that this mechanism is more applicable in the case where surface metal cations are easily accessible for gas-phase $CH_3^{\bullet}$ radicals, e.g., a partially reduced metal oxide surface. On partially

---

(24) Garibyan, T.; Margolis, L. Ya. *Catal. Rev. - Sci. Eng.* **1989-90**, *31*, 355–384.

(25) Kung, H. H. Transition Metal Oxides: Surface Chemistry and Catalysis. In *Studies in Surface Science and Catalysis*; Delmon, B., Yates, J. T., Eds.; Elsevier: New York, 1989; Chapter 6.

(26) Grunze, M.; Hirschwald, W.; Thuuull, E. *Phys. Chem. N. F.* **1976**, *100*, 201.

(27) Bell, R. P. *The Tunneling Effect in Chemistry*; Chapman and Hall: New York, 1980; p 63–67.

(28) Bockris, J. O'M.; Wass, J. *J. Electroanal. Chem.* **1989**, *267*, 329–332.

(29) Zamaraev, K. I.; Khairutdinov, R. F. *Sov. Sci. Rev., Sect. B* **1980**, *2*, 357–469.

(30) Goldfeld, M. G.; StreKova, L. N.; Khairutdinov, R. F. *Proc. 13th Int. Conf. Photochem.*, Budapest, 1987; p 430.

(31) Somorjai, G. A. *Chemistry in Two Dimensions Surfaces*; Cornell University Press: New York, 1981; p 27–30.

(32) Li, T. T.-T.; Weaver, M. J. *J. Am. Chem. Soc.* **1985**, *106*, 6107–6108.

(33) Jwo, J.-J.; Hain, A. *J. Am. Chem. Soc.* **1976**, *98*, 1172–1176.

(34) Durante, V. A.; Ford, P. C. *J. Am. Chem. Soc.* **1975**, *97*, 6898–6900.

reduced MoO_3, the removal of surface oxide ions would increase the possibility for gas-phase $CH_3{}^{\bullet}$ radicals to access the Mo^{6+} ions, which previously were located under those 4-fold oxide ions.

Molecular orbital calculations have been carried out by Anderson and co-workers[35-37] concerning the adsorption of $CH_3{}^{\bullet}$ radicals on metal oxides, such as MoO_3 and MgO. One conclusion from these studies is that, generally, surface metal cations can form stronger bonds with methyl radicals than do surface oxide ions. Compared with the preceding mechanism, the preference of the gas-phase methyl radicals for metal ions, instead of O^{2-}, upon adsorption may be accounted for by the ease of electron transfer directly from the carbon to the metal ion. The electron transfer from the carbon of methyl radicals to metal cations is expected only for those metal ions that have accessible multiple oxidation states. The extent of the electron transfer is determined by the reducibility of the metal cations; that is, the more easily an oxide can be reduced, the more the carbon is charged. The Coulombic interaction between the positively charged carbon and the negatively charged O^{2-} is believed to be the driving force for the migration of the methyl radical from the metal cation to the O^{2-} anion. It is apparent that the greater the charge on the carbon of the adsorbed methyl radicals, the stronger the interaction will be.

Another factor that needs to be considered is the extent of adsorption of methyl radicals on the metal cations of a metal oxide. As concluded from the calculations of Anderson and co-workers,[35-37] the carbon–metal bond formed upon the adsorption of methyl radicals on metal cations may not be strong enough to survive under the conditions for the oxidative dimerization of methane. Thus, the adsorbed methyl radicals would desorb from the metal cations before they undergo any surface reaction. This is consistent with the fact that most of methyl–metal complexes are stable only under mild conditions, such as at ambient temperature or even lower. Since the experiments of this study were carried out under severe conditions (>450 °C and 10^{-2} Torr), the formation of the $H_3C^{\delta+}M^{(n+1-\delta)+}O^{2-}$ complexes was not favorable. That is, the decomposition of the complex to yield methyl radicals was fast compared with the migration to an oxide ion. This implies a small sticking coefficient since according to this model the sticking coefficient is just the ratio of the migration rate to the sum of the migration rate and the desorption rate. The argument here is similar to that in the case of the dissociative adsorption of nitrogen molecules on Fe surfaces where sticking coefficients of 10^{-6}–10^{-7} are typical.[38]

The rapid desorption and the slow migration results in an adsorption–desorption equilibrium

$$CH_3{}^{\bullet}{}_{(g)} + O^{2-}M^{(n+1)+} \rightleftarrows H_3C^{\delta+}M^{(n+1-\delta)+}O^{2-} \qquad (11)$$

followed by migration of the CH_3 group:

$$H_3C^{\delta+}M^{(n+1-\delta)+}O^{2-} \rightarrow M^{n+}(OCH_3)^{-} \qquad (12)$$

The low activation energies for the overall reaction also can be interpreted through this mechanism. The apparent activation energy derived from the reaction scheme is

$$E_a = E_{12} - Q_{11} \qquad (13)$$

where $Q_{11} = E_{-11} - E_{11}$ is the heat of adsorption for the equilibrium 11 and E_{12} is the activation energy for reaction 12. Equation 13 implies that the stronger the M–CH_3 bond, i.e., the larger the heat of adsorption, the lower will be the apparent activation energy, E_a. A strong bond between the metal cation and the methyl radicals would lead to a high concentration of the intermediate species and consequently a high rate of reaction 10. This is consistent with the fact that methyl ligands can form stronger bonds with transition-metal cations than with Group IA and IIA metal cations, and consequently, transition-metal oxides are generally more reactive than Group IA and IIA metal oxides. The weak dependence of the reaction rate on temperature is a result of a compensation effect. That is, any increase in temperature results in an enhancement in the rate constant of reaction 12, but on the other hand a decrease in the concentration of surface methyl groups results in a shift in equilibrium 11.

Conclusion

Large differences occur in the reactivities of $CH_3{}^{\bullet}$ radicals with metal oxides. Those metal oxides in which the cations exhibit accessible multivalent oxidation states are highly reactive. The reactions of $CH_3{}^{\bullet}$ radicals with a metal oxide can be described by a mechanism in which metal cations are reduced as a result of the electron transfer from $CH_3{}^{\bullet}$ radicals to the metal cations. The resulting methoxide and formate ions are intermediates for the oxidation of the $CH_3{}^{\bullet}$ radicals to CO_x and H_2O.

The reactions of $CH_3{}^{\bullet}$ radicals with metal oxides are characterized by small activation energies and small sticking coefficients. Two alternative mechanisms have been proposed to interpret these observations. In one of the mechanisms, the electrons on weakly adsorbed $CH_3{}^{\bullet}$ radicals tunnel through the oxide ions and reduce the metal ions in the proximity of the surface. According to the other mechanism, a $CH_3{}^{\bullet}$ radical is initially adsorbed on a metal cation with a partial electron transfer. The adsorbed $CH_3{}^{\bullet\delta+}$ species then moves to a neighboring oxide ion as a result of a Coulombic interaction between the positively charged $CH_3{}^{\bullet}$ radical and the oxide ion.

Acknowledgment. We acknowledge financial support of this work by the Division of Chemical Sciences, Office of Basic Energy Sciences, U.S. Department of Energy.

---

(35) Mehandru, S. P.; Anderson, A. B.; Brazdil, J. F. *J. Phys. Chem.* **1987**, *91*, 2930–2934.

(36) Mehandru, S. P.; Anderson, A. B.; Brazdil, J. F. *J. Am. Chem. Soc.* **1988**, *110*, 1715–1719.

(37) Mehandru, S. P.; Anderson, A. B.; Brazdil, J. F. *J. Chem. Soc., Faraday Trans. 1* **1987**, *83*, 463–475.

(38) Ertl, G. Primary Steps in Ammonia Synthesis. *Proc. of the Robert A. Welch Foundation, Conferences on Chemical Research, XXV. Heterogeneous Catalysis*, Houston, 1981; pp 179–217.